Transaction A: Civil Engineering
Vol. 16, No. 6, pp. 502–511

Failure Criteria of Unreinforced Grouted Brick Masonry Based on a Biaxial Compression Test

B. Badarloo[1], **A.A. Tasnimi**[1,*] **and M.S. Mohammadi**[1]

Abstract. *To define failure under biaxial stress, a three-dimensional surface in terms of two principal stresses and their orientation to the bed joints is required. This article describes a series of biaxial compression tests on full-scale brick specimens. Tests were performed on square unreinforced grouted brick masonry specimens with the principal compressive stresses oriented at 0 and 90 degree angles to the bed joints, and a failure surface was obtained in terms of these parameters. Test results indicated that the masonry strength under equal biaxial compression is higher by about 36% on average than that under uniaxial compression; the influence of joint orientation is very insignificant and negligible for these models.*

Keywords: *Failure criteria; Masonry panel; Principal stress; Biaxial stresses; Bed joints.*

INTRODUCTION

Most masonry structures are subjected to a complex state of stress during their lifetime. Shear walls, infill walls in frame structures and walls supported by beams etc. are in a state of biaxial stress when subjected to in-plane loading. Based on the location of masonry panels within a building, biaxial stress states can be Compressive-Compressive State (CCS), Compressive-Tensile State (CTS) and Tensile-Tensile State (TTS). Little emphasis has been placed on the development of a fundamental theory of failure that could be applied to any case of in-plane loading. Computer-based numerical techniques have made the need for this information more pressing, as the definition of local failure is of prime importance in modeling masonry behavior realistically. Masonry exhibits distinct directional properties because of the influence of the unit's arrangement and the mortar joints, which act as planes of weakness. Its failure cannot therefore be defined simply in terms of a criterion based on the principal stresses at any point. The influence of bed joint orientation relative to principal stresses is the main variable that must also be taken into account. Depending on the orientation of the joints to the applied stresses, failure can occur in the joints alone or in some form of combined mechanism involving mortar and the masonry unit. Thus, to define masonry failure completely, a three-dimensional failure surface in terms of the principal stresses, σ_1 and σ_2, and their respective orientations to the bed joint of 0 and 90° is required. To derive this surface, biaxial tests must be performed to cover the CCS, CTS and TTS principal stress domains. In practice, the most critical regions are those of CTS and CCS.

This paper reviews research carried out at the Structural Laboratory in Tarbiat Modares University (TMU) on the biaxial strength of masonry and describes an investigation into the biaxial strength of full-scale brick masonry. This involved biaxial compression tests on square grouted brick masonry specimens with varying principal stress ratios and bed joint orientations. The study forms part of a series of tests aimed at developing a complete (σ_1, σ_2, θ) failure surface for all principal stress combinations.

PREVIOUS RESEARCH

For a long time, the significance of joint orientation to the stress state of masonry panels has been of interest to many researchers. Johnson and Thompson [1] described diametral tests on brick masonry discs, which produced indirect tensile stresses on joints inclined at various angles to the compressive load. Similar tests on grouted and un-grouted concrete masonry have been reported by Drysdale and Hamid [2]. The influence

1. *Department of Civil Engineering, Tarbiat Modares University, Tehran, P.O. Box 14155-143, Iran.*
*. *Corresponding author. E-mail: tasnimi@modares.ac.ir*

Received 28 February 2009; received in revised form 11 July 2009; accepted 31 August 2009

of bed joint orientation has also been shown in many investigations carried out into shear wall behavior [3]. There have been few attempts to obtain a general failure criterion for masonry because of the difficulty in developing a representative biaxial test, as well as the large number of tests involved. The problem has been qualitatively discussed by Yokel and Fatta1 [4] and Hendry [5]. Samarasinghe [6] and Samarasinghe and Hendrye [7] obtained a $(\sigma_1, \sigma_2, \theta)$ failure surface for the tension-compression principal stress range from tests on one-sixth scale brickwork. Page [8-10] studied the behavior of brick masonry under biaxial CCS, CTS and TTS of stresses. He proposed failure surfaces for the three biaxial stress cases in which he observed that the bed joint orientation has little influence on the shape of the failure surface for the case of CCS, but exerts significant influence under the CTS and TTS of stress. Also, it was found that bed joint orientation affected the failure pattern only when one of the principal stresses dominated. Similar observations were also made by Samarasinghe [6] on the behavior of brick masonry under biaxial compression-tension. The proposed failure surfaces were in terms of principal stresses and bed joint orientation. Ganz and Thurlimann [11], Ganz [12] and Dhanasekar et al. [13] proposed failure surfaces in terms of orthogonal stresses and shear stress. The influence of joint orientation has been found to be less significant for grouted concrete masonry. From a comprehensive series of biaxial tests on full-scale grouted concrete masonry (both reinforced and un-reinforced), Hegemier et al. [14] found the influence of the bed joint angle to be minimal and the behavior essentially isotropic. However, this isotropy could be destroyed by improper selection of block and grout strengths. Lourenco [15] developed a material model for masonry that combined the modern plasticity concepts (hardening, softening, flow rule and evolution laws) with an anisotropic behavior along each material axis. During the past decade, very limited research has been carried out on the behavior of reinforced and unreinforced brick masonry under biaxial stress states. Alshebani and Sinha [16] investigated the behavior of brick masonry under a pseudo dynamic (cyclic) biaxial stress state. Naraine and Sinha [17] studied the behavior of brick masonry under cyclic biaxial compression and obtained that masonry under cyclic biaxial compression can exhibit three distinct stress-strain curves; they proposed a generalized interaction formula for this failure in terms of stress invariant for the range of stress ratios considered. Also, Senthivel and Uzoegbo [18] experimentally investigated the failure criterion of unreinforced masonry under biaxial pseudo dynamic loading. They proposed a general analytical expression for the envelope interaction curves, common point interaction curves and stability point interaction curves. They suggested that by assigning suitable values for equation parameters, the expression could be used to determine the peak stress of the envelope curve, the common point curve and the stability point curve. The aim of this research is to produce the failure criteria of unreinforced grouted brick masonry panels, for the purpose of a design process. This paper describes the tests carried out on square grouted unreinforced brick masonry panels with the principal compressive stresses oriented at 0 and 90 degree angles to the bed joints, and a failure surface was obtained in terms of these parameters.

EXPERIMENTAL PROGRAM

The experimental program involved testing full-scale grouted unreinforced brick masonry panels under monotonic biaxial loading that induced a CCS of stress. The angle of inclination between the horizontal principal stresses and the bed joints was limited to 0° and 90°. Five principal stress ratios were considered for the investigation as $\frac{f_n}{f_p} = 0, 0.2, 0.5, 1, 2, 5$ where f_n and f_p are the applied stresses normal to the bed joint ($\theta = 90°$) and parallel to the bed joint ($\theta = 0°$), respectively.

Description of Test Specimens

This paper presents an experimental program of testing seven masonry full-scale grouted unreinforced brick masonry specimens under monotonic biaxial compression. All panel specimens were constructed with three layers, consisting of one single wythe of $221.9 \times 110 \times 68.5$ mm solid clay bricks, one single wythe of $204.7 \times 58.5 \times 54.9$ mm clay hollow bricks and a 51.5 mm thick grout layer between the brick wythes. The overall dimension of each panel was $950 \times 95 \times 220$ mm from which a central area of 600×600 mm^2 was selected for measurement. To identify specimens, they were nominated mainly by four characters for specimens under uniaxial compression, and three characters followed by one or two digits corresponding to the normal to parallel stress ratio for specimens under biaxial compression. For example, the brick panel, under the uniaxial compression load ($f_n = 0$) parallel to the bed joint is named UPCP, and that under biaxial compression with ($\alpha = \frac{f_n}{f_p} = 0.2$) is named BPC02. Table 1 summarizes all specimens with their relevant states of stress.

A chemical admixture was used to compensate for shrinkage and enhance the workability of the grout. The grout was placed using internal vibration to obtain good consolidation. To ensure uniform workmanship, all test specimens were constructed by the same mason and were cured under damped conditions for 28 days before testing. The overall size of the fabricated specimens was 950 mm × 950 mm × 220 mm. Generally,

Table 1. Specimens identification corresponding to their loading state.

Specimen Name	State of Applied Load	f_n	f_p	$\alpha = f_n/f_p$
UPCP	Uniaxial compression parallel to bed joint	-	$\surd$	-
UPCN	Uniaxial compression normal to bed joint	$\surd$	-	-
BPC1	Equal biaxial compression	$\surd$	$\surd$	1
BPC2	Biaxial compression	$\surd$	$\surd$	2
BPC05	Biaxial compression	$\surd$	$\surd$	0.5
BPC5	Biaxial compression	$\surd$	$\surd$	5
BPC02	Biaxial compression	$\surd$	$\surd$	0.2

solid clay bricks are used for masonry brick building, infill panels etc., and hollow clay bricks are used for the finishing of brick masonry (face brick) walls in the country. For convenience, the solid clay brick and the hollow clay brick are, hereafter, referred to as C-Brick and F-Brick, respectively.

Material Properties

Quality control samples were obtained for the mortar, grout, C-Bricks, F-Bricks and the masonry units during the construction of all specimens.

The mortar mix proportions was an ASTM C270-92 type-S mortar, comprised of 1 part Portland cement, 5.81 parts sand and 0.9 parts water by weight. Fifteen mortar 50 mm cube specimens were made from each mortar mix and tested after 28 days for compressive strength as per ASTM C-109-92.

The average mortar compressive strength obtained from cube compression tests was 12.46 MPa.

The grout mix proportions were an ASTM C476-02 of 1 part type-I Portland cement, 3.68 parts sand, 2.25 parts 12 mm nominal maximum-size broken stone, 0.018 parts of a commercial chemical admixture (Sika Grout-Aid) and 0.8 parts water by weight. Six grout 100 mm cube specimens were made from each grout mix and tested after 28 days for compressive strength, as per ASTM C1019-02. The average grout compressive strength obtained from cube compression tests was 22.84 MPa.

In order to evaluate the compressive strength of masonry, fifteen 4-course masonry prisms (couplet specimens) were tested, as per ASTM C-1314-02a. The average prism compressive strength was 4.0 and 6.4 MPa for the F-Brick and C-Brick prisms, respectively. The average compressive strength of ten C-Bricks and ten F-Bricks was 34 and 32.6 MPa, respectively. The average compressive strength of masonry prisms is less than the average compressive strength of the used C-Bricks, F-Bricks and mortar. This is attributed to the failure mechanism of masonry prisms in which the vertical splitting of the bricks is occurred prior to the crushing of the mortar. In other words, the vertical splitting of the bricks due to the different material properties of the bricks and mortar leads to a premature failure of the prisms. This is because the higher Poisson ratio of the mortar results in a tendency for lateral mortar tensile strains to exceed lateral brick strains [19]. Therefore, the normal compression and lateral biaxial tension in the bricks reduces its crushing strength and induces a tendency for vertical splitting. In such situations, the vertical splitting strength of the bricks was less than the compressive strength of the bricks and that of mortar. This phenomenon indicates the failure of bricks in the form of vertical splitting prior to the failure of prisms in compression.

As no ASTM testing procedures exist for shear strength determination, the modified triplet specimen for pure shear was used to obtain the mortar shear strength and friction coefficient [20]. This specimen represents the actual shear loading case of masonry walls along the mortar bed-joints. The value of the brick-mortar interface bond strength (mortar shear bond strength) was 0.451 Mpa and the average coefficient of friction of the mortar joint was 0.65.

To evaluate the flexural bond strength of C-Brick and F-Brick masonry, seven and eight 5-course masonry units were tested as per ASTM C1072-00a. The average flexural bond strength was 2.52 and 1.96 MPa for the C-Brick and H-Brick masonry units, respectively.

According to the ASTM C1314-02a, the compressive strength of seven 4-course masonry panel prisms (couplet specimens) was carried out and the average panel prism compressive strength obtained as 7.1 MPa. Table 2 summarizes the properties of each specimen and Figure 1 illustrates the geometry and dimensions of the test specimens

Loading Arrangement

The test setup, including a specimen, reaction ring and the monotonic biaxial loading arrangement (CCS), is shown in Figure 2. The biaxial steel ring was designed so that the maximum deformation under a prospective maximum load would be negligible. A

Table 2. Summary of result of auxiliary assemblages after 28 days.

Specimen Number	Test Type				
	Compression (MPa)		Flexural (MPa)		Compression (MPa)
	C-Brick	F-Brick	C-Brick	F-Brick	Panel Prism
1	5.5	4.4	2.29	2.23	6.7
2	5.7	3.8	2.64	1.94	5.8
3	5.7	4.5	3.31	1.67	8.2
4	6.0	2.6	2.42	2.03	5.8
5	9.7	3.5	1.87	1.99	8.1
6	6.1	5	1.76	1.73	7.9
7	5.6	4.4	2.72	2.12	7.5
8	6.8	-	3.19	-	-
Average	6.4	4.0	2.52	1.96	7.1

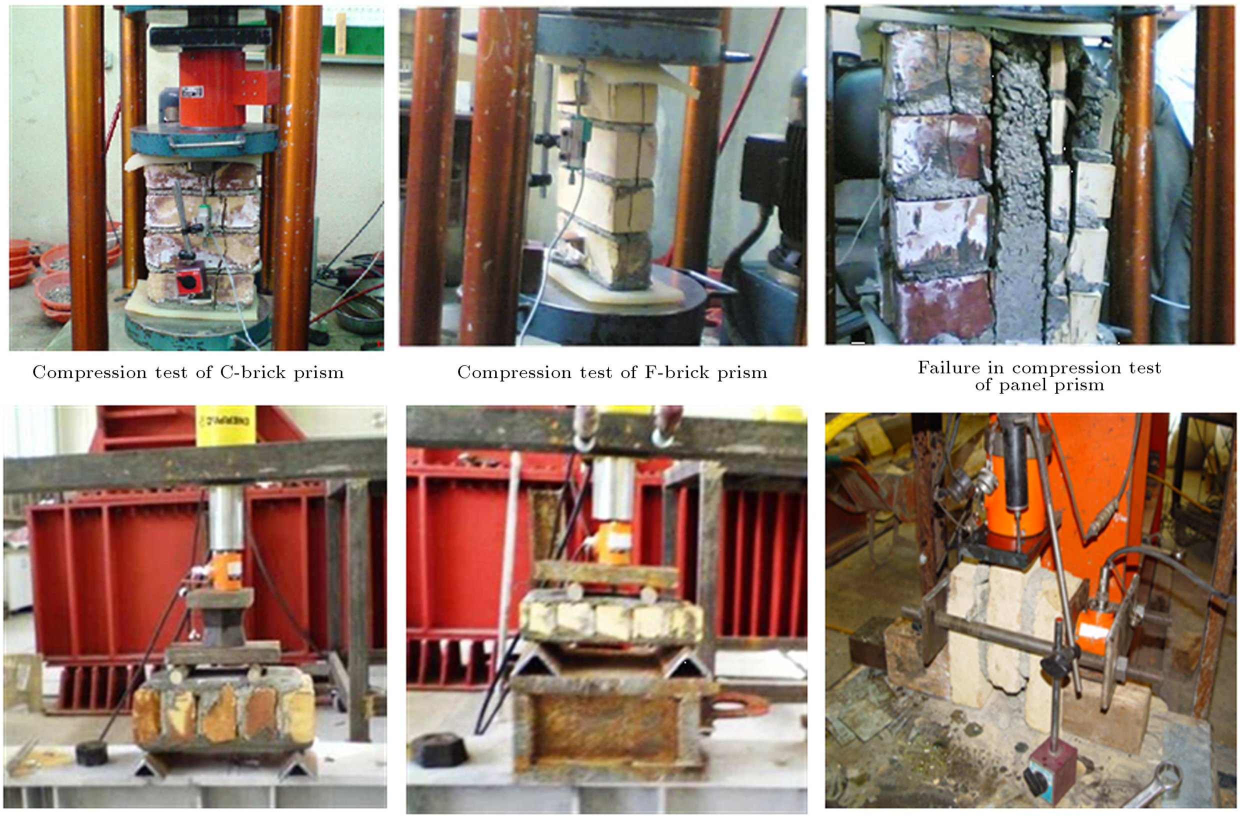

Compression test of C-brick prism

Compression test of F-brick prism

Failure in compression test of panel prism

Flexural tensile test of C-brick masonry unit

Flexural tensile test of F-brick masonry unit

Shear test of C-brick masonry unit

Figure 1. Test setup and failure of auxiliary assemblages.

biaxial state of stress was achieved by applying in-plane loads with the use of two double-acting hydraulic actuators aligned in two orthogonal directions as shown in Figure 2. The capacity of each hydraulic actuator is 3000 kN for both compression and tension. The load measurement was carried out by installing two load cells placed in line with the central axes of the panel and connected to a data-logger system of type TML. In order to apply a distributed load to the specimen, a steel rigid beam made of PL850 $\times$ 250 $\times$ 30 mm in I-section, which was sufficiently stiffened with PL850 $\times$ 250 $\times$ 10 mm vertical stiffeners, was utilized (Figure 3a). This rigid beam was used as a loading platen on four sides of the specimen. When the masonry panel specimen is subjected to biaxial compression loads, it may be under confining pressure

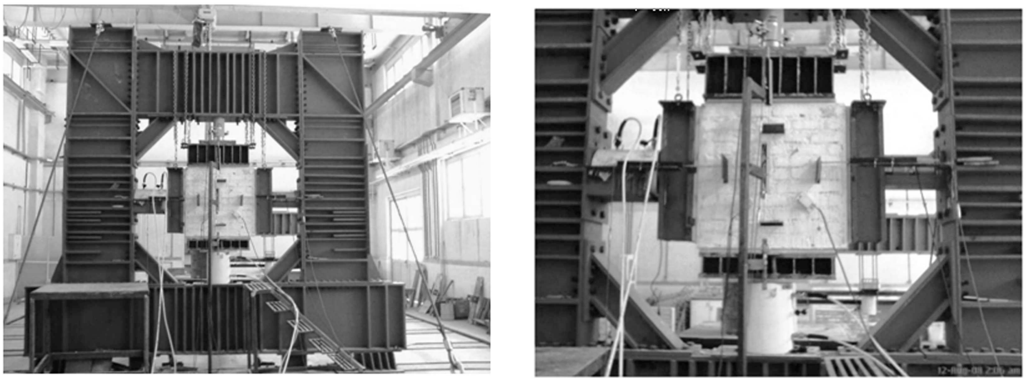

Figure 2. General setup for biaxial tests.

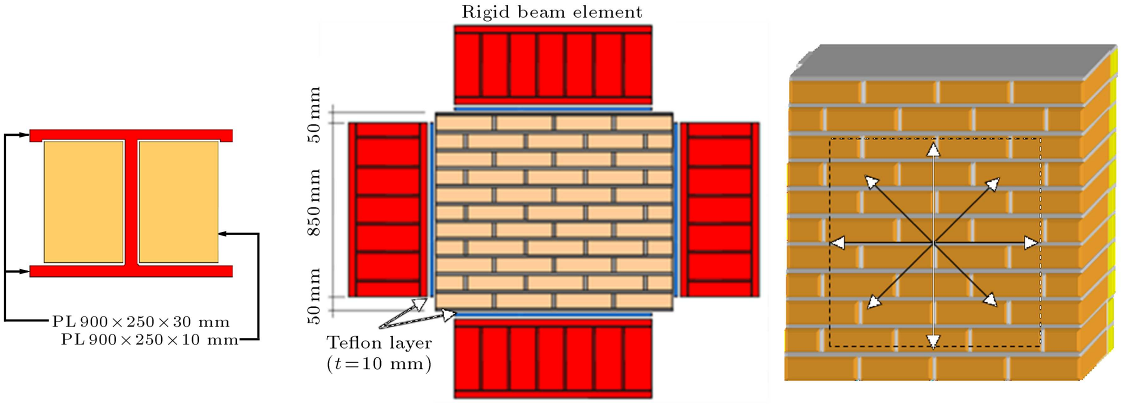

(a) Detail of rigid beam section (b) Loading platens with Teflon pads around specimen (c) LVDTs arrangement

Figure 3. Schematic arrangement and geometry of masonry panel specimen.

along its loaded surfaces due to friction between the solid platens of the test setup and the masonry panel's bearing surface. The effect of such restraint may result in an increase of the apparent strength of the test specimen [21-24]. To minimize such a confinement of the specimen due to friction and thus to ensure a more uniform state of stress is imposed on the specimen, 10 mm thick Teflon pads were used on all four bearing surfaces of the brick masonry panel. Figure 3b shows a schematic arrangement of loading platens, a masonry panel and Teflon pads mounted between them. To avoid unexpected additional confinement, due to the contact of adjoining plates, when the specimen is under biaxial compression, the width of the loading plates was 850 mm (100 mm less than the specimen width).

INSTRUMENTATION

The masonry specimens were instrumented with LVDTs (linearly variable displacement transducers) aligned in two principal directions and two diagonal directions on the C-Brick surface of the panel as shown in Figure 3c. The LVDTs were installed to measure the axial, lateral and diagonal displacements over a fixed gauge length. The gauge lengths of 600 mm, 600 mm and 450 mm were adopted for the measurement of axial, lateral and orthogonal deformations, respectively. A data-logger system was used to display, monitor and record the load and displacement measurements in real time during the test. The ratio between horizontal and vertical loads was controlled in the real time of the test.

RESULTS

A total of 7 specimens, including two uniaxial and five biaxial compression specimens, were tested. For specimens under biaxial compressive stresses, different ratios of stress normal to the bed joint (f_n) to the stresses parallel to the bed joint (f_p), were used in two groups. For the first group, the ratios of 1, 2, 5 and ∞ were used for bed joint angles of 0° and 90° with respect to the horizontal axis. For the second group, the results corresponding to the ratios of 0, 0.2 and 0.5 were obtained on the basis of symmetry of the specimens and loading conditions. The following paragraphs describe the failure mode, crack propagation and the failure criterion of all specimens.

Failure Modes

The crack patterns and failure modes of both layers observed in the specimens after failure varied markedly with the relative proportions of the applied stresses. Figure 4 shows photographs of the failure modes that were observed for all the stress ratios considered in this investigation. Failure of the specimen UPCP indicates an extensive crushing of the C-brick layer and, at some portion of the panel, the bricks were separated from the mortar at the bed joints (Figure 4a). Failure of the F-brick layer of this specimen exhibited vertical cracking over the entire height of the panel.

In the case of specimen UPCN, the failure of the C-brick layer exhibited major diagonal cracks with different depths at different parts. In some regions, diagonal cracks passed through the thickness of the C-Brick layer and reached the interface plane between the grout layer and the C-Brick layer (Figure 4b). The F-brick layer disparted from the central grout layer up to the mid-height of the specimen. A series of micro cracks on the F-brick layer is observed.

In the case of equal stress ratio ($\alpha = 1$), the failure of specimen BPC1 was indicated by the separation of C-brick and F-brick layers from the middle grout layer. The strength of this specimen is almost 36% higher than that under uniaxial compression.

As shown in Figure 4c, the failure of specimen BPC2 is indicated by increasing the width of the diagonal and vertical cracks in the C-brick layer. At the same time, both the C-brick and F-brick layers were partially separated from the middle grout layer. Also, the failure of the F-brick layer resulted from the propagation of diagonal cracks over the entire height of the specimen, which was followed by complete separation from the middle grout layer (Figure 4d). Failure of specimen BPC05 under biaxial compression ($\alpha = 0.5$) was initiated by the formation of vertical cracks on the upper portion of the F-brick layer and followed by the crushing of the C-brick layer at one side of the panel, which is illustrated in Figure 4e. The main cause of this phenomenon was the splitting of this layer from the middle grout layer at the free edge, which gradually propagated towards the center of the specimen. For high stress ratio ($\alpha = 5$), the specimen BPC5 displayed a typical mode of failure due to the crushing of the C-brick layer, which separated from the grout layer at the upper half part of the panel (Figure 4f). The spalling failure of the F-brick layer occurred suddenly in a brittle manner and often begins

Figure 4. Failure modes of masonry specimens under different stress ratios.

by vertical cracking at one of the loaded edges, which propagates into the panel height.

The failure of specimen BPC02, tested under biaxial compression with low stress ratio ($\alpha = 0.2$), was indicated by the crushing of the C-brick layer on the left-side of the panel and embarked on its splitting from the grout layer as shown in Figure 4g. Thereafter, the separated fragments of the panel behave like individual compression members. The failure of the F-brick layer of this specimen is shown in Figure 4h.

Due to the high compression strength of the grout layer compared to that of F-brick and C-brick layers, the middle grout layer experienced no serious damage for all specimens. The reason for this phenomenon is firstly related to the high compression strength of the grout in comparison with the compression strength of the masonry prisms and, secondly the bonding weakness at the interface of the C-brick, F-brick and the grout layer. It seems that the effect of the second factor is more considerable.

Failure Surface

The in-plane failure of masonry can be presented either in terms of a principal stress system (σ_1, σ_2, θ) or a stress state related to the bed joint (f_n, f_p, τ). A failure surface in terms of one of these stress sates may be transformed into the alternative failure surface. The failure envelopes obtained for each bed joint angle ($\theta =$ 0°, 90°) are illustrated in Figure 5. The envelope for $\theta = 90°$ is obtained by interchanging f_n and f_p in the 0° envelope.

The failure surface curves are plotted in a non-dimensional form as shown in Figure 6. These curves have been normalized with respect to uniaxial compressive strength (f'_m) for normal loads, to the bed joint ($\theta = 0°$). f'_m is the mean compressive strength of 7 samples of panel prisms. This value was determined at full scale using the same construction and curing techniques as for the masonry panels. σ_n and σ_p represent the non-dimensional stress parameters. The values of σ_n and σ_p are obtained by normalizing f_n and f_p with respect to the failure (peak) stress (f'_m) of each specimen.

As shown in Figure 6, the failure envelope for bed joint orientations (0° and 90°) have a reasonably good fit with each other. Based on the results obtained in this investigation, it seems that the influence of bed joint orientation has a minor effect on the behavior and failure criteria of the tested specimens.

Failure Criterion

The accuracy of the yield surface obtained experimentally is validated by comparing it with the simplest yield surface that features different compressive strengths along the material axes. The simplest yield surface is a rotated centered ellipsoid in the full plane stress space (σ_x, σ_y and τ_{xy}). This is illustrated in Figure 7. Equation 1 expresses the general two-dimensional yield criteria relevant to such a quadratic:

$$f = A\sigma_x^2 + B\sigma_x\sigma_y + C\sigma_y^2 + D\tau_{xy}^2 - 1 = 0, \qquad (1)$$

where A, B, C and D are four material parameters. In order to ensure the convexity of the surface, these material parameters should satisfy $B^2 - 4AC < 0$.

$$A = \frac{1}{f_{mx}^2}, \qquad B = \frac{\beta}{f_{mx}.f_{my}},$$

$$C = \frac{1}{f_{my}^2}, \qquad D = \frac{\gamma}{f_{mx}.f_{my}}.$$

It should be noted that the parameters β and γ introduced in the above are additional material parameters that determine the shape of the yield surface [15].

Parameter β controls the coupling between the normal stress values, i.e. rotates the yield surface around the shear stress axis, and must be obtained from

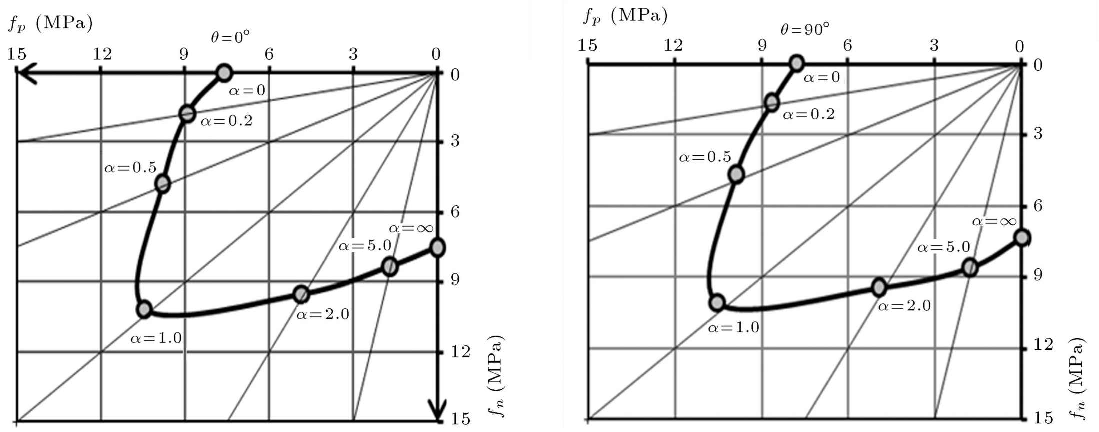

Figure 5. Failure of masonry panel under biaxial compression.

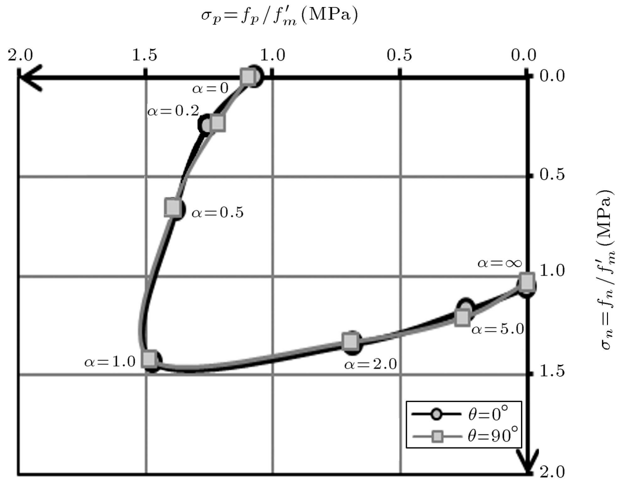

Figure 6. Failure surface curves in a non-dimensional form.

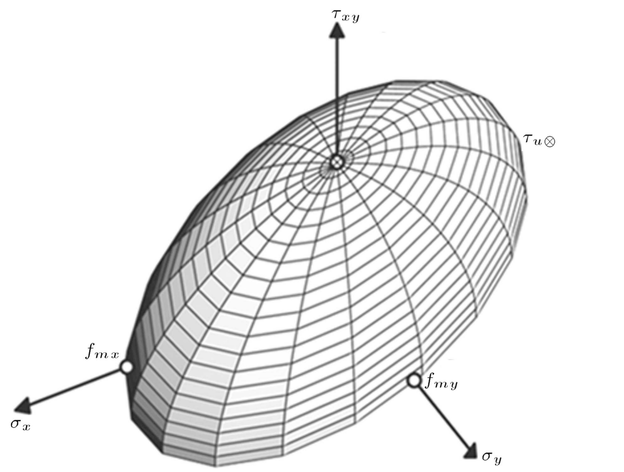

Figure 7. The Hill type yield surface (shown for $\tau_{xy} \geq 0$).

one additional experimental test, e.g. biaxial compression with a unit ratio between principal stresses; its value can be obtained from the following equation:

$$\beta = \left(\frac{1}{f_\beta^2} - \frac{1}{f_{mx}^2} - \frac{1}{f_{my}^2}\right) f_{mx}.f_{my}. \qquad (2)$$

Parameter γ which controls the shear stress contribution to failure can be obtained from Equation 3:

$$\gamma = \left[\frac{16}{f_\gamma^2} - 9\left(\frac{1}{f_{mx}^2} - \frac{\beta}{f_{mx}^2} - \frac{1}{f_{my}^2}\right)\right] f_{mx}.f_{my}. \qquad (3)$$

All parameters, f_{mx}, f_{my}, β and γ, can be determined by the uniaxial and biaxial experiments illustrated in Figure 8.

In this investigation, the only masonry models with bed joint orientations of 0° and 90° were investigated, so the term relevant to shear stress would be zero and, hence the evaluation of γ is not required. Therefore, Equation 1 yields to the simple form given by Equation 4:

$$f = Af_x^2 + Bf_xf_y + Cf_y^2 - 1 = 0. \qquad (4)$$

Based on the results obtained experimentally, the evaluated parameters, f_{mx}, f_{my} and β, are 7.6, 7.5 and -1.464, respectively. Figure 9 illustrates reasonable correlation between experimental failure curves and the Hill failure criteria. From a qualitative perspective, good agreement is found, because the same trend is observed in both diagrams.

CONCLUSIONS

This paper describes a series of uniaxial and biaxial tests on full-scale grouted unreinforced brick masonry square panels. A failure criterion, with the principal compressive stresses oriented at 0° and 90° angles to the bed joints, is obtained. The following conclusions have been drawn.

The ratio of the horizontal to the vertical load has significant influence on the failure mode of the C-brick and F-brick layers of panels, while it has little influence on the failure mode of the grout layer. The ratio of the loading has a significant influence on the ultimate force of the specimens. The fundamental failure mode of all specimens corresponding to the loading ratio was splitting the grout layer from the C-brick or F-brick layer. The results obtained from this research show that the

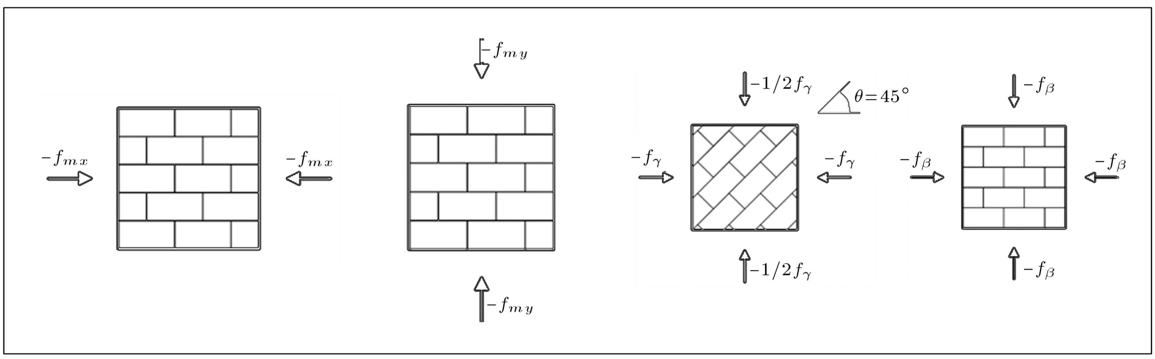

Figure 8. Tests to obtain the values of f_{mx}, f_{my}, β and γ parameters.

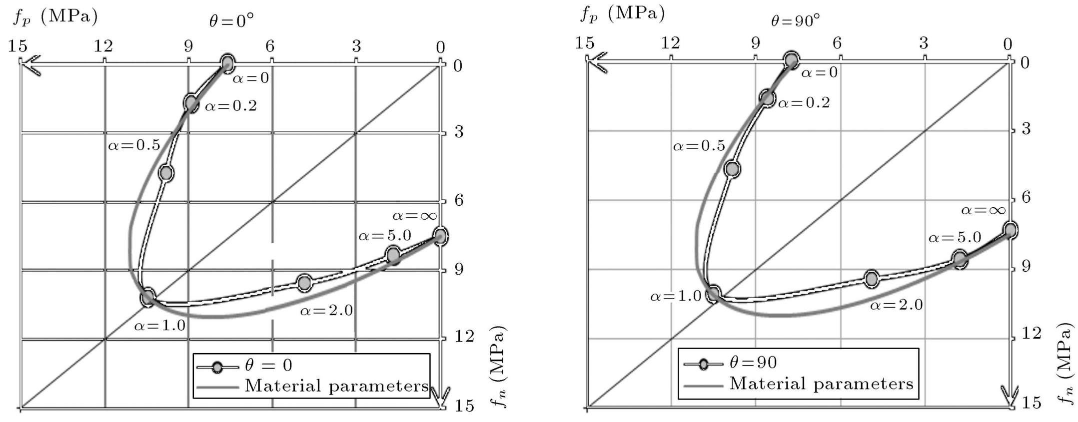

Figure 9. Comparison between experimental and Hill criteria.

behavior of grouted unreinforced brick masonry panels was isotropic and the bed joint orientation did not play a significant role in the failure criterion. The comparison between experimental failure and HILL criteria exhibits reasonable agreement. From a qualitative perspective, a good agreement was obtained because the same trend is observed in both criteria.

NOMENCLATURE

f_n	principal stress normal to bed joint
f_p	principal stress parallel to bed joint
f'_m	uniaxial compressive strength for load normal to the bed joint
β, γ	material parameters determining the shape of the Hill yield surface

REFERENCES

1. Johnson, F.B. and Thompson, J.N. "Development of diametric testing procedures to provide a measure of strength characteristics of masonry assemblages", *Designing, Engineering and Constructing with Masonry Products*, F.H. Johnson, Ed., pp. 51-57, Gulf Publishing, Houston (1969).
2. Drysdale, R.G. and Hamid, A.A. "Behavior of concrete block masonry under axial compression", *American Concrete Institute Journal*, **76**(6), pp. 707-721 (1979).
3. Page, A.W. et al. "The in-plane failure of masonry-an overview", *Proc. 7th Int. Symp. Load Bearing Brickwork*, London (1980).
4. Yokel, F.Y. and Fattal, J.G. "Failure hypothesis for masonry shear walls", *Journal of Structural Division, ASCE*, **102**(ST3), pp. 515-532 (1976).
5. Hendry, A.W.A. "Note on the strength of brickwork in combined racking shear and compression", *Proc. Brit. Ceram. Soc.*, **27**(6), pp. 47-52 (1978).
6. Samarasinghe, W. "The in-plane failure of brickwork", PhD thesis, University of Edinburgh (1980).
7. Samarasinghe, W. and Hendry, A.W. "The strength of brickwork under biaxial tension-compression", *Proc. 7th International Symposium on Load Bearing Brickwork*, London, pp. 129-140 (1980).
8. Page, A.W.A. "Biaxial failure criterion of brick masonry in the tension-tension range", *Inter. Journal of Masonry Construction*, **1**(1), pp. 26-29 (1980).
9. Page, A.W. "The biaxial compressive strength of brick masonry", *Proc. of the Institution of Civil Engineers*, **71**(2), pp. 893-906 (1981).
10. Page, A.W. "The strength of brick masonry under biaxial compression-tension", *Inter. Journal of Masonry Construction*, **3**(1), pp. 26-31 (1983).
11. Ganz, H.R. and Thurlimann, B. "Strength of brick walls under normal force and shear", *Proc. of the 8th International Symposium on Load Bearing Brickwork*, London, pp. 27-29 (1983).
12. Ganz, H.R. "Failure criteria for masonry", *Proc. of the 5th Canadian Masonry Symposium*, pp. 65-77 (1989).
13. Dhanasekar, M. et al. "The failure of brick masonry under biaxial stresses", *Proc. of the Institution of Civil Engineers*, Part 2, pp. 295-313 (1985).
14. Hegemier, A. et al. "Behavior of concrete masonry under biaxial stress", *Proc. of the North American Masonry Conference*, Boulder, University of Colorado, pp. 1-10 (1978).
15. Lourenco, P. "Computational strategies for masonry structures", Dissertation, TU Delft, Delft, the Netherlands (1996).
16. Alshebani, M.M. and Sinha, S.N. "Cyclic biaxial stress-strain curves of masonry: A generalized approach", *Journal of Structures & Buildings*, **146**(2), pp. 141-145 (2000).
17. Naraine, K. and Sinha, S.N. "Stress-strain curves for brick masonry in biaxial compression", *Journal of Structural Engineering, ASCE*, **118**(6), pp. 1451-1461, (1992).
18. Senthivel, R. and Uzoegbo, H.C. "Failure criterion of unreinforced masonry under biaxial pseudo dynamic loading", *Journal of the South African Institution of Civil Engineering*, **46**(4), pp. 20-24 (2004).

19. Paulay, T. and Priestley, M.J.N., *Seismic Design of Reinforced Concrete and Masonry Buildings*, John Wiley & Sons, Inc., New York, USA (1992).

20. Harris, H.G. and Sabnis, G.M., *Structural Modeling and Experimental Techniques*, CRC Press, New York, USA (1999).

21. Kupfer, H. and Hilsdorf, H.K. "Behavior of concrete under biaxial stress", *ACI J. Proc.*, **66**(8), pp. 656-666 (1969).

22. Vile, G.W.D. "Strength of concrete under short-time static biaxial stress", *Proc. of the International Conference of the Structure of Concrete*, Paper F2 (1965).

23. Sundara, R., Iyengar, K.T. et al. "Strength of concrete under biaxial compression", *ACI J. Proc.*, **62**(2), pp. 239-249 (1965).

24. Robinson, G.S. "Behavior of concrete in biaxial compression", *Proc. ASCE*, **93**(ST1), pp. 71-86 (1967).